Articles

Intrazeolite Photochemistry. 26. Photophysical Properties of Nanosized TiO_2 Clusters Included in Zeolites Y, β, and Mordenite

S. Corrent,[†] G. Cosa,[†] J. C. Scaiano,*[,†] Maria S. Galletero,[‡] Mercedes Alvaro,[‡] and H. Garcia*[,‡]

Department of Chemistry, Centre for Catalysis Research and Innovation, University of Ottawa, Ottawa, Ontario, Canada K1N 6N5, and Instituto de Tecnología Química, Universidad Politécnica de Valencia, Apartado 22012, 46071 Valencia, Spain

Received October 25, 1999. Revised Manuscript Received November 13, 2000

The photophysical properties of TiO_2 included in zeolites Y, β, and mordenite are determined using time-resolved techniques. The shift in the ground-state absorption spectra for the TiO_2−zeolite samples, compared to bulk phase anatase, is attributed to a direct transition in the semiconductor, based on calculated electronic transition energies. Excitation of the samples at 355 nm results in the formation of a trapped electron. Time-resolved fluorescence spectra are dependent upon the sample treatment, that is, whether the sample is heated prior to monitoring of the emission. Significant changes were found in the emission λ_{max} and decay kinetics. These changes that occur are due to the presence of two different Ti species in the nanoclusters, differing in the presence of hydroxyl groups bonded to Ti atoms, that in turn depends on the thermal treatment and the relocation/redistribution of water around the Ti atoms. Changes in relative intensities between the two sets of samples are attributed to defect sites that are produced upon heating of the sample at high temperatures.

Introduction

Studies of titanium dioxide have received much attention in recent years.[1−12] It has been used as a photocatalyst in many applications, including degradation of pollutants and solar energy conversion, as well as in the transformation of organic compounds. The mechanism for TiO_2-mediated degradation involves its oxidative/reductive capabilities. Excitation of TiO_2 with light of energy greater than the band gap results in electron ejection from the semiconductor valence band, generating a positive hole and a conduction band (CB) electron. This process occurs on the femtosecond time scale.

Many studies on the photocatalytic properties of TiO_2 have been performed, frequently aiming at improving its catalytic efficiency. The structure of the photocatalyst plays a vital role. Thus, studies of TiO_2 anchored on Vycor glass[13] or doped with transition metals[6] have been done in an effort to gain control of the catalytic efficiency of bulk anatase.

The incorporation of TiO_2 in zeolite cavities offers a new design of a photocatalytic system. This is due to the nanoscaled pores that zeolites contain, along with their ion-exchange capabilities that allow the preparation of clusters of TiO_2 of tailored dimensions within a rigid environment of variable polarity and hydrophilicity, and where other cooperating sites can be present. There have been earlier reports on the incorporation of TiO_2 inside zeolite cages[14−17] or anchored to the surface

[†] University of Ottawa.
[‡] Universidad Politécnica de Valencia.

(1) Trentler, T. J.; Denler, T. E.; Bertone, J. F.; Agrawal, A.; Colvin, V. A. *J. Am. Chem. Soc.* **1999**, *121*, 1613.
(2) Colombo, D. P., Jr.; Bowman, R. M. *J. Phys. Chem.* **1995**, *99*, 11752.
(3) Draper, R. B.; Fox, M. A. *Langmuir* **1990**, *6*, 1396.
(4) Morris Hotsenpiller, P. A.; Bolt, J. D.; Farneth, W. E.; Lowekamp, J. B.; Rohrer, G. S. *J. Phys. Chem. B.* **1998**, *102*, 3216.
(5) Zhang, Z.; Wang, C.-C.; Zakaria, R.; Ying, J. Y. *J. Phys. Chem.* **1998**, *102*, 10871.
(6) Martin, S. T.; Morrison, C. L.; Hoffmann, M. R. *J. Phys. Chem.* **1994**, *98*, 13695.
(7) Emeline, A. V.; Ryabchuk, V. K.; Serpone, N. *J. Phys. Chem. B* **1999**, *103*, 1316.
(8) Serpone, N.; Lawless, D.; Khairutdinov, R.; Pelizzetti, E. *J. Phys. Chem.* **1995**, *99*, 16655.
(9) Hoffman, M. R.; Martin, S. T.; Choi, W.; Bahnemann, D. W. *Chem. Rev.* **1995**, *95*, 69.
(10) Inoue, T.; Fujishima, A.; Konishi, S.; Honda, K. *Nature* **1979**, *277*, 637.
(11) Heller, A. *Acc. Chem. Res.* **1995**, *28*, 503.
(12) Ishitani, O.; Inoue, C.; Suzuki, Y.; Ibusuki, T. *J. Photochem. Photobiol. A: Chem.* **1993**, *72*, 269.
(13) Anpo, M.; Aikawa, N.; Kubokawa, Y.; Che, M.; Louis, C.; Giamello, E. *J. Phys. Chem.* **1985**, *89*, 5017.
(14) Yamashita, H.; Ichihashi, Y.; Anpo, M.; Hashimoto, M.; Louis, C.; Che, M. *J. Phys. Chem.* **1996**, *100*, 16041.
(15) Yamashita, H.; Fujii, Y.; Ichihashi, Y.; Zhang, S. G.; Ikeue, K.; Park, D. R.; Koyano, K.; Tatsumi, T.; Anpo, M. *Catal. Today* **1998**, *45*, 221.
(16) Liu, X.; Iu, K.-K.; Thomas, J. K. *J. Chem. Soc., Faraday Trans.* **1993**, *89*, 1861.

10.1021/cm990679+ CCC: $20.00
Published on Web 02/21/2001

of the zeolite.[17−19] These reports have focused primarily on the photocatalytic properties of these systems, such as the reduction of CO_2 with H_2O.[20,21] Some time-resolved measurements have also been reported,[16] but we could find no reports on the time-resolved fluorescence of such systems. Time-resolved measurements that determine the photophysical properties of a system can also be vital for determining the structure of the TiO_2 clusters and their homogeneity and can help anticipate the photocatalytic efficiency of these materials, leading to the preparation of more active and selective photocatalysts. For example, the active sites in the alkene epoxidation catalyzed by Ti-containing zeolites are due to tetrahedrally coordinated framework Ti. The presence of octahedrally coordinated Ti is inactive toward such reactions, due to a lack of free coordination sites.[22]

This report focuses on pico−nanosecond fluorescence measurements of samples of TiO_2 included in zeolites Y, β, and mordenite. The effect of heating the samples at 300 °C (referred to as "baked samples") is examined, and the results are compared to those of samples that have been stored at room temperature (referred to as "air-equilibrated samples"). Significant changes in intensity, emission wavelength, and decay kinetics were found, dependent upon the sample history. The fluorescence was studied over the period of 1 month, to monitor any changes due to aging. Assignments of the absorption bands are given, based on theoretical calculations of the electronic band structure of TiO_2.[23]

To analyze the electronic band structure of crystals, the Brillouin zone of the crystal is employed. The unit cell of TiO_2 is tetragonal, and the Brillouin zone is also tetragonal, which is defined in space by vectors. The edge of the Brillouin zone is represented by X and the center of the zone is represented by Γ, using the notation of Daude et al., who have calculated the band structure of TiO_2. The nature of the lowest allowed transition in the Brillouin zone will aid in classifying semiconductor materials. The lowest allowed transition for semiconductors consists of a transition from the maximum of the valence band to the minimum of the conduction band. For TiO_2, the valence band is mainly composed of O^{2-} 2p states and the conduction band consists of the 3d states of Ti^{4+}.

All semiconductors are classed as either direct or indirect semiconductors. A direct semiconductor is one in which the nature of the lowest allowed transition[24] occurs from the same point in the Brillouin zone. The maximum of the valence band and minimum of the conduction band are either both at the center of the Brillouin zone, Γ, or both at the edge of the Brillouin zone, X. Thus, a direct transition would occur from $X_a \rightarrow X_b$ or from $\Gamma_a \rightarrow \Gamma_b$.

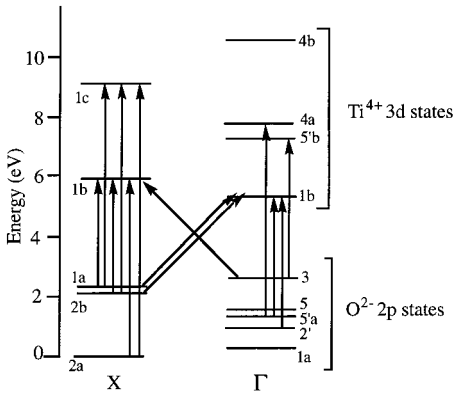

Figure 1. Energy level diagram showing the relative energy levels in TiO_2 as calculated by Daude et al.[23] A few of the direct and indirect transitions are illustrated.

For an indirect semiconductor, the class to which TiO_2 belongs, the maximum of the valence band and the minimum of the conduction band occur at different points in the Brillouin zone, Γ and X. That is, the maximum of the valence band may be located at the edge of the Brillouin zone, while the minimum of the conduction band is located at the center of the Brillouin zone, or vice versa. Thus an indirect transition would be from X → Γ or Γ → X. Direct transitions in an indirect semiconductor can still occur, but the energies associated with them will always be greater than the band gap energy. Radiative recombination in an indirect semiconductor is possible, but this process is not as efficient compared to a direct semiconductor. Figure 1 illustrates some of these transitions in TiO_2.

Controversial reports in the literature have debated whether the quantum size effect for nanoparticles of TiO_2 is applicable or not; in contrast, for other semiconductors such as CdS nanoparticles quantum size effects have been more convincingly established.[25] A quantum size effect was invoked to explain the shift in the absorption spectra of nanosized particles of TiO_2, compared to bulk anatase. This interpretation leads to the conclusion that there is a change in the band gap energy. By using the effective mass model approach (EMM), a size determination of the nanoparticles can be made, based on the blueshift in the absorption spectrum.[26,27] The other side to this debate argues that there is no size quantization for nanoparticles of $TiO_2 > 4$ nm; the band gap is the same as that in bulk anatase.[28] The blueshift seen in the absorption spectra would be, then, attributed to a direct transition in the indirect semiconductor. While the controversy about quantum effects continues and our work does not address this important issue, it is worth noting that TiO_2 clusters embedded within the zeolite micropores ($\leq$1.3 nm) would be in the ideal size range in which this effect could be observed.

(17) Fox, M. A.; Doan, K. E.; Dulay, M. T. *Res. Chem. Intermed.* **1994**, *20*, 711.
(18) Xu, Y.; Langford, C. H. *J. Phys. Chem. B* **1997**, *101*, 3115.
(19) Xu, Y.; Langford, C. H. *J. Phys. Chem.* **1995**, *99*, 11501.
(20) Anpo, M.; Yamashita, H.; Ichihashi, Y.; Fujii, Y.; Honda, M. *J. Phys. Chem. B* **1997**, *101*, 2632.
(21) Kim, Y. I.; Keller, S. W.; Krüger, J. S.; Yonemoto, E. H.; Saupure, G. B.; Mallouk, T. E. *J. Phys. Chem. B* **1997**, *101*, 2491.
(22) Marchese, L.; Maschmeyer, T.; Gianotti, E.; Coluccia, S.; Thomas, J. M. *J. Phys. Chem. B* **1997**, *101*, 8836.
(23) Daude, N.; Gout, C.; Jouanin, C. *Phys. Rev. B* **1977**, *15*, 3229.
(24) Davies, J. H. *The Physics of Low-Dimensional Semiconductors: An Introduction*; Press Syndicate of the University of Cambridge: Cambridge, 1998.
(25) Logunov, S.; Green, T.; Marguet, S.; El-Sayed, M. A. *J. Phys. Chem. A* **1998**, *102*, 5652.
(26) Kormann, C.; Bahnemann, D. W.; Hoffmann, M. R. *J. Phys. Chem.* **1988**, *92*, 5196.
(27) Choi, W.; Termin, A.; Hoffmann, M. R. *J. Phys. Chem.* **1994**, *98*, 13669.
(28) Serpone, N.; Lawless, D.; Khairutdinov, R. *J. Phys. Chem.* **1995**, *99*, 16646.

Experimental Section

Preparation of Samples for Time-Resolved Measurements. Formation of TiO_2 clusters inside the zeolite micropores was accomplished by ion exchange using aqueous solutions of commercial $(TiO)K_2(C_2O_4)_2 \cdot H_2O$ (Aldrich) and subsequent mild calcination/polymerization at 150 °C for 8 h as previously reported.[16] Characterization data based on FT-Raman spectroscopy showed the disappearance of $Ti{=}O^{2+}$ and the formation of TiO_2 clusters with bands in the 540 cm^{-1} region, similar to those of anatase. Surface area measurements by isothermal nitrogen adsorption (Micrometrics) indicated a significant decrease after formation of the TiO_2 clusters. This could be attributed to either partial pore filling or pore blockage by the generated TiO_2 clusters. Thermogravimetry coupled with differential scanning calorimetry, (Netzsch thermobalance operated under air stream using kaolin as inert standard) revealed that the amount of coadsorbed water present under stationary conditions on the TiO_2-containing zeolites was about 5 wt % for all of the samples. This value is remarkably lower than the regular water content of the original zeolites (approximately 25, 20, and 15 wt % for zeolite Y, β, and mordenite, respectively). Thus, formation of TiO_2 nanoclusters clearly reduces the amount of coadsorbed water for zeolites Y, mordenite, and β, respectively.

The TiO_2−zeolite samples were divided in two portions. One portion (referred to as baked sample) was heated at 300 °C for 18 h, then placed on a vacuum line (P = 30 mTorr), and sealed. No special handling precautions were used with the other portion of the samples (referred to as air-equilibrated samples throughout the paper). For a few preliminary laser flash photolysis experiments, the TiO_2−zeolite samples used were the air-equilibrated ones.

Instrumentation. Ground-state diffuse-reflectance spectra were recorded on a Cary 1E spectrophotometer. Steady-state fluorescence spectra were recorded on an Edinburgh FL-500 spectrofluorimeter. Laser flash photolysis experiments were carried out using a time-resolved, diffuse-reflectance setup, similar to that developed by Wilkinson and co-workers.[29−31] Picosecond fluorescence measurements were carried out using a Hamamatsu C-4334 streakscope coupled with a spectrograph capable of simultaneous spectral and time-resolved data acquisition.[32] A 375 nm cutoff filter was used to avoid any scattered light from the excitation beam to reach the detector. The excitation source was the third harmonic of a Continuum PY-61 Nd/YAG laser (355 nm, <4 mJ/pulse, 150 ps full width at half-maximum (fwhm) pulse). The kinetic data were fitted with biexponential functions using the Hamamatsu software package. Control experiments with pristine Y, β, and mordenite zeolites did not show significant emission under the conditions employed in this work.

Sample Preparation. Clusters of TiO_2 inside the micropores of zeolites were prepared by starting from the Na^+ form of the corresponding zeolite and ion-exchanging the Na^+ by $Ti{=}O^{2+}$ according to the reported procedure. Formation of TiO_2 clusters is subsequently achieved by moderate heating (150 °C) of the TiO^{2+}-exchanged zeolite in the presence of moisture according to eq 1.

$$TiO^{2+} + H_2O \rightarrow TiO_2 + 2H^+ \quad (1)$$

This cycle consisting of TiO^{2+} ion exchange and heating was repeated three times in order to achieve zeolites with higher TiO_2 loadings.

Given that the internal location of the charge-balanced cations is well-established, the Na^+-to-TiO^{2+} ion exchange ensures the internal location inside the micropores of the $Ti{=}O^{2+}$. Although migration of atomic cluster to the external surface of the zeolite could occur upon heating at high temperatures, the moderate heating used in the present work makes this process very unlikely.

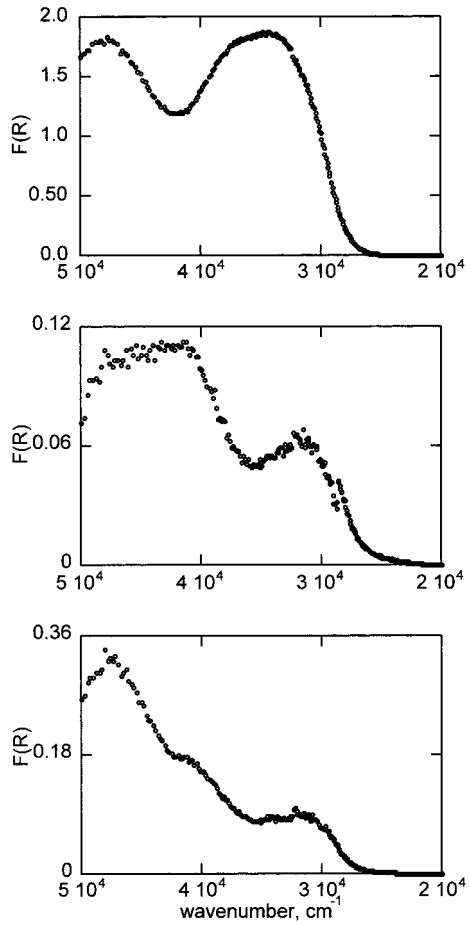

Figure 2. Ground-state absorption spectra for TiO_2 included in zeolites Y (top), mordenite (middle), and β (bottom)

Results

Absorption Spectroscopy. The ground-state absorption spectra of the air-equilibrated samples of TiO_2 included in zeolites Y, β, and mordenite are shown in Figure 2, plotted as a function of wavenumber. The absorption onset for the three samples, which are the same as the baked ones, are at 3.4 eV for TiO_2 in Y and 3.6 eV for TiO_2 in zeolites β and mordenite. These values are different than the absorption onset for bulk anatase, which occurs at 3.2 eV.[23]

Transient Absorption Spectroscopy. Exploratory diffuse-reflectance laser flash photolysis (DR-LFP) of the samples of TiO_2 in zeolites, using an excitation wavelength of 355 nm, was performed. The transient absorption spectrum for the sample of TiO_2 in zeolite Y has a broad absorption from 550 to 750 nm, with a λ_{max} centered at ~650 nm. The other TiO_2−zeolite samples also displayed a broad transient absorption, but its center is blueshifted by ~100 nm, with some absorption still occurring at 650 nm. This could be attributed to reduced Ti^{3+} species that are produced shortly after irradiation. The decay traces indicate a long-lived species, and in fact, a nonzero baseline is seen even 20 μs after the laser pulse.

(29) Wilkinson, F.; Willsher, C. J. *Appl. Spectrosc.* **1984**, *38*, 897.
(30) Wilkinson, F.; Willsher, C. J.; Casal, H. L.; Johnston, L. J.; Scaiano, J. C. *Can. J. Chem.* **1986**, *64*, 539.
(31) Wilkinson, F.; Kelly, G. In *Handbook of Organic Photochemistry*; J. C. Scaiano, Ed.; CRC Press: Boca Raton, FL, 1989; Vol. 1; p 293.
(32) Mohtat, N.; Cozens, F. L.; Scaiano, J. C. *J. Phys. Chem. B* **1998**, *102*, 7557.

Table 1. Lifetimes and Weight Factors for Samples of TiO_2 in Zeolites Y, β, and Mordenite[a]

		blue spectral region		red spectral region	
zeolite	TiO_2 sample	τ_1(ps), (A1)	τ_2 (ps), (A2)	τ_1(ps), (A1)	τ_2 (ps), (A2)
Y	baked	<pulse, (0.61)	932 (0.39)	188 (0.55)	1107 (0.45)
	air-equilibrated	<pulse, (0.69)	964 (0.31)	<pulse (0.64)	1129 (0.36)
	baked aged sample	<pulse (0.73)	1116 (0.27)	<pulse (0.72)	1160 (0.28)
mordenite	baked	<pulse (0.77)	981 (0.23)	<pulse (0.66)	1060 (0.34)
	air-equilibrated	<pulse (0.57)	1217 (0.43)	<pulse (0.61)	1190 (0.39)
	baked, aged sample	177 (0.52)	1441 (0.48)	<pulse (0.63)	1283 (0.37)
β	baked	<pulse (0.71)	1007 (0.29)	<pulse (0.48)	1160 (0.62)
	air-equilibrated	<pulse (0.71)	1030 (0.29)	<pulse (0.65)	1206 (0.35)
	baked, aged sample	176 (0.57)	1206 (0.43)	169 (0.57)	1401 (0.43)

[a] The blue and red regions of the emission were monitored separately, and each region was fitted as a biexponential decay. The blue spectral regions are centered at 400, 407, and 402 nm and have widths of 61, 52, and 46 nm for zeolites Y, mordenite, and β, respectively. The red spectral regions are centered at 528, 526, and 503 nm and have widths of 200, 180, and 150 nm for zeolites Y, mordenite, and β, respectively.

Luminescence Measurements. Excitation of the samples at 290 nm produced a weak steady-state luminescence with λ_{max} at 390 nm. Time-resolved fluorescence measurements on the zeolite samples following 355 nm laser excitation displayed an emission λ_{max} between 440 and 455 nm, with the emission extending past 550 nm. We were concerned that this emission could be due either to trace amounts of organic compounds that are frequently adsorbed in high surface-solids such as zeolites or to artifacts from the cells or due to light scattering. To rule out these possibilities, we recorded the luminescence of the original Y zeolite using the same experimental procedure. Under these conditions, we were in fact able to detect some luminescence, but the intensity of the emission (obtained by integration of the area of this control spectrum) was 2 orders of magnitude lower than the emission from the TiO_2-containing zeolites.

Spectral features were highly dependent upon the sample conditioning (i.e., those baked at 300 °C and then vacuum sealed, or those air-equilibrated) as well as on the time window selected for the emission (i.e., within the laser pulse, or significantly after the laser pulse). These significant changes between the two sets of samples prompted us to examine the time-resolved emissions over an aging period in excess of 1 month, to monitor any time-dependent changes. The fluorescence decay kinetics for all of the zeolite samples were adequately fitted by a biexponential decay. The fits obtained for all of the samples under the different conditions started at 100 ps after the laser pulse and ended at 1.6 ns after the laser pulse.

The fluorescence intensity for the zeolite samples was generally fairly weak. For TiO_2 incorporated in zeolite Y, heating of the sample causes a significant change in the emission spectra, as can be seen in Figure 3. The air-equilibrated sample, when the full emission range is examined (not shown in the figure), has a broad peak centered at ~460 nm. Examination of the time windows during the laser pulse, (instrument response 130 ps) and well after the pulse has ended (from 580 to 5700 ps), shows a shift in λ_{max}, from 440 to 472 nm. Heating of the sample at 300 °C results in an emission spectrum, followed by spectroscopy at room temperature, that has a much sharper peak, with λ_{max} centered at 450 nm, irrespective of the time window being monitored. There is also some emission at longer wavelengths (>520 nm). In addition, the lifetimes and pre-exponential factors

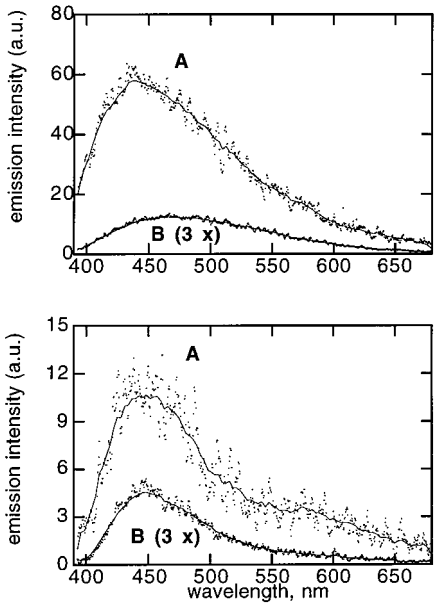

Figure 3. Time-resolved emission spectra of TiO_2 in zeolite Y: air-equilibrated (top) and baked (bottom) samples. Lines: **A**, time window during the laser pulse, and **B**, time window taken between 580 and 5700 ps.

for the emission decays vary between the baked and air-equilibrated samples of TiO_2 in zeolite Y. These values are given in Table 1. It should be noted that the emission intensity of the air-equilibrated sample was much higher than that for the baked sample. Two components are observed for the decay: one with a lifetime shorter than, or equal to the instrument response, and a slower one, with a lifetime of approximately 1.1 ns. When monitoring the decays as a function of wavelength, there is a clear increment in weight of the faster component with a decrease in the monitoring wavelength for the air-equilibrated sample. This clear progression is lost after baking, when the weight of both components is independent of the wavelength. The presence of these two components can be assigned to two different species (vide infra) with very similar emission spectra.

The sample of TiO_2 in mordenite also showed major changes in the emission spectra when comparing baked and air-equilibrated samples, but they showed a different trend compared to the emission of TiO_2 in zeolite Y. Thus, the emission for the air-equilibrated TiO_2-mordenite sample showed a single λ_{max} at 450 nm,

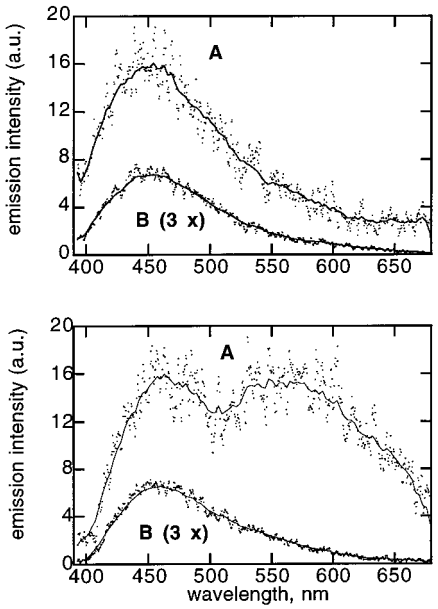

Figure 4. Time-resolved emission spectra of TiO_2 included in mordenite: air-equilibrated (top) and baked (bottom) samples. Lines: **A**, time window during the laser pulse, and **B**, time window taken between 580 and 5700 ps.

regardless of the time window being monitored, whereas TiO_2−Y displayed two λ_{max} for the air-equilibrated sample (see above). The emission is still fairly broad, with some emission extending past 520 nm. Upon baking of the sample, instead of obtaining a sharper emission peak, as was seen for TiO_2 in zeolite Y, a much broader emission occurs, with two resolvable peaks being detected for emission occurring within the laser pulse. Compared to the air-equilibrated sample, the emission intensity is much higher at longer wavelengths (λ > 500 nm). The spectra for these two sets of samples are shown in Figure 4. The lifetimes also varied with monitoring wavelength for the baked sample, with a difference of >200 ps for emission in the red and blue spectral regions. This is best illustrated in Figure 5, which contains the decay traces for the baked and air-equilibrated samples. In contrast to what was seen for TiO_2 in zeolite Y, the intensity of the baked sample for TiO_2 in mordenite was greater than that for the air-equilibrated sample.

The sample of TiO_2 in zeolite β, on the other hand, did not show such major differences between air-equilibrated and baked samples, as occurred with the other zeolite samples. Both sets of samples displayed an emission λ_{max} at ∼450 nm, with little emission intensity at longer wavelengths. The overall emission intensity of the baked sample was much less than the air-equilibrated sample, which was also seen in the case of TiO_2 in zeolite Y. Some changes were noted in the lifetimes between the two sets of samples.

For all of the zeolite samples studied, one trend was apparent: upon examination of the baked samples throughout a period of 1 month, the spectral features became similar to those observed for the air-equilibrated samples. This illustrates that the process being monitored in the baked sample is a reversible one. This holds true not only for the spectral features, but also for the decay kinetics. The spectra of the baked samples that have aged for 1 month are given in Figure 6 for samples

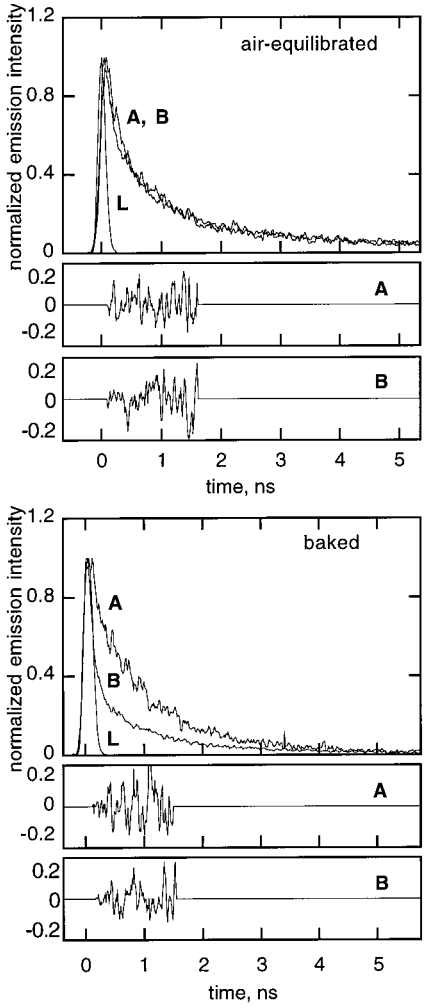

Figure 5. Fluorescence decay traces for TiO_2 in mordenite: air-equilibrated (top) and baked (bottom) samples. Lines: **L**, laser pulse; **A**, decay taken in the blue region of the spectrum (see Table 1); and **B**, decay taken in the red region of the spectrum (see Table 1). Lower sections: plots of residuals.

of TiO_2 in mordenite and in zeolite Y. It is worth mentioning that the emission intensities cannot directly be compared when acquisitions are taken on different days; only the relative intensities of spectra taken on the same day can be compared. The lifetimes measured for these samples, which varied according to sample conditioning, can be generalized in the following manner: Two components were measured, one with a very short lifetime (approximately within the laser pulse) and the second with a lifetime of around 1 ns, for both the blue and red spectral regions.

Discussion

Ground-State Absorption Spectra. The ground-state absorption onset for TiO_2 included in three different zeolites occurs at 3.4 eV for TiO_2 in zeolite Y and at 3.6 eV for TiO_2 in mordenite and in β zeolites. The size and shape of the TiO_2 clusters in the zeolites are expected to differ between zeolite Y, containing spherical cages and mordenite, which has a channel structure. This is reflected in the significant change in the onset of absorption for TiO_2 in these two zeolites, suggesting that the zeolite structure does have an effect in controlling the shape of the TiO_2 particles. This has been seen

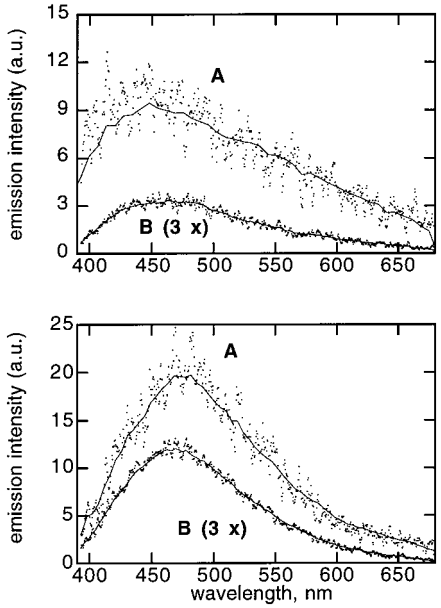

Figure 6. Time-resolved emission of baked TiO_2 samples in zeolite Y (top spectra) and mordenite (bottom spectra). These samples have aged for 1 month. Note the similarities in the spectra to those of the air-equilibrated samples shown in Figures 3 and 4. Lines: **A**, time window within the laser pulse, and **B**, time window taken from 580 to 5500 ps.

in other work done on TiO_2 included in zeolites[16] where differences in absorption onsets were observed for zeolites containing different pore structures.

The differences in the onset of the ground state absorption, which is blueshifted compared to the value for bulk anatase, do not necessarily imply that the band gap energies for the nanoparticles are different. Rather, the absorption onset values for TiO_2 in the three zeolite samples refer to direct transitions in TiO_2 from $X_{1a} \rightarrow X_{1b}$ and $X_{2b} \rightarrow X_{1b}$ that have calculated energies of 3.49 and 3.59 eV, respectively.[23] The absorption onset for bulk anatase occurs at 3.2 eV, corresponding to the indirect transition $\Gamma_3 \rightarrow X_{1b}$, which is the band gap energy. These results correlate well with those of Serpone et al.[28] for TiO_2 nanoparticles with diameters in the 2−27 nm range.

Formation of Trapped Electrons. The broad absorption in the region of 550−750 nm in the transient absorption spectra of TiO_2 in zeolite Y is characteristic of the trapped electron, probably in the form of Ti^{3+} species seen in other systems.[2,8,33] The diffuse-reflectance transient absorption spectra for TiO_2 in mordenite and β zeolite are also broad, with their maxima shifted with respect to the zeolite Y sample. The broad absorption is also assigned to the trapped electron that is produced following excitation. The species that may ultimately trap the electron is either Ti^{4+} or the zeolite countercation. This results in the formation of Ti^{3+} or Na or K cationic clusters, respectively. (Note: K^+ cation is also introduced in zeolite Y during the ion exchange with $(TiO)K_2(C_2O_4)_2$ used in the present experiments.) The exact nature of the trapped electron cannot be distinguished at the present time. For example, the absorption of Na_4^{3+} clusters has been reported in zeolite Y as a broad band at 500−550 nm, depending on the Si/Al ratio of the sample.[34,35] The absorption spectrum of K_4^{3+} is very similar but somewhat redshifted.[36,37] The transient absorption spectra that we obtain for the TiO_2−zeolite samples are fairly broad, and thus no accurate determinations of the formation of alkali metal cationic clusters can be made. The fluorescence studies, on the other hand, proved significantly more informative in understanding the behavior of TiO_2 nanoclusters in zeolites.

Interpretation of Luminescence Data. Standard TiO_2 samples of micrometer particle size in the anatase or rutile phases do not emit or show a very weak emission at $\lambda_{max} \sim 500$ nm ($\lambda_{fwhm} = 100$ nm). In contrast, colloidal TiO_2 powders (40 Å particle size) exhibit much stronger emission at λ_{max} between 360 and 450 nm depending on the aging and thermal treatment.[38−40] There have also been luminescence studies of Ti atoms occupying positions in the framework of the zeolite structure. One such example is Ti−silicalite where the location and coordination of framework Ti atoms have been studied by luminescence measurements combined with other techniques such as XANES and IR.[22,41] Through these studies, it was determined that there are two different framework Ti atoms in the zeolite, as could be seen by the two different emission wavelengths of 430 and 500 nm. It was also determined that framework Ti, in a tetrahedral coordination, upon interaction with a ligand such as water, expands the coordination sphere of Ti(IV), appearing as a titanol group (Ti−OH) that shows a distinctive emission compared with Ti atoms lacking OH groups in their coordination sphere.[41] A return back to the initial tetrahedral coordination of Ti occurs upon prolonged outgassing at room temperature. These findings, particularly the different emission λ_{max} of titanol lumophores compared to the rest of Ti atoms not bonded to OH groups, are valuable in the interpretation of the characteristics of TiO_2 nanoclusters in zeolites and the reversible changes occurring upon baking.

By applying these observations to our results, it is reasonable to assume that the changes in spectral features between baked and air-equilibrated samples are due to two different Ti species, where the difference lies in the coordination sphere of the octahedral Ti atoms, that is, the presence or absence of Ti(OH) sites. To explain the significant changes in intensity between baked and air-equilibrated samples, an additional argument must be invoked, which is most likely due to a structural change in the TiO_2 nanocluster upon heating.

The thermal annealing of the crystal surface of TiO_2 using a temperature >200 °C was found to produce

(33) Rabani, J.; Yamashita, K.; Ushida, K.; Stark, J.; Kira, A. *J. Phys. Chem. B* **1998**, *102*, 1689.

(34) Iu, K.; Liu, X.; Thomas, J. K. *J. Phys. Chem.* **1993**, *97*, 8165.
(35) Liu, X.; Iu, K.; Thomas, J. K. *J. Phys. Chem.* **1994**, *98*, 13720.
(36) Liu, X.; Zhang, G.; Thomas, J. K. *J. Phys. Chem.* **1995**, *99*, 10024.
(37) Liu, X.; Thomas, J. K. *J. Chem. Soc., Faraday Trans.* **1995**, *91*, 759.
(38) Liu, Y.; Claus, R. O. *J. Am. Chem. Soc.* **1997**, *119*, 5273.
(39) Monticone, S.; Tufeu, R.; Kanaev, A. V. *Chem. Phys. Lett.* **1998**, *295*, 237.
(40) Nakato, Y.; Tsumura, A.; Tsubomura, H. *J. Phys. Chem.* **1983**, *87*, 2402.
(41) Bordiga, S.; Coluccia, S.; Lamberti, C.; Marchese, L.; Zecchina, A.; Boscherini, F.; Buffa, F.; Genoni, F.; Leofanti, G.; Petrini, G.; Vlaic, G. *J. Phys. Chem.* **1994**, *98*, 4125.

defect sites on the crystal surface.[42] The nature of the defect site was suggested to be the cleavage of the bridging oxygen atom, resulting in the exposure of two Ti^{3+} cations. It was also shown that adsorbed D_2O, CH_2O, and NO molecules are reduced at the defect sites to produce D_2, C_2H_4, and N_2O, respectively. The deoxygenation of adsorbates is accompanied by the oxidation of surface Ti^{3+} sites. The creation of defect sites upon heating the TiO_2−zeolite samples would result in lower emission intensity. This is a logical consequence of the nature of the emission band, which is generally assumed to be a charge-transfer state from $(Ti^{3+}-O^-)^*$, in the case of tetrahedrally coordinated Ti.

To fully explain all of the changes that occur upon baking of the TiO_2−zeolite samples, a combination of two arguments will be used. The first one is that through emission spectroscopy it is possible to detect two different Ti species: one which is free of water and the other which has water as a ligand. Thermogravimetry of the TiO_2-containing zeolites reveals that air-equilibrated samples contain ca. 5 wt % of coadsorbed water. We believe that the presence or removal of water is responsible for the shifts in the emission wavelengths. The second argument, which explains the reduction in intensity of the baked samples, is the formation of defect sites that occurs upon sample heating. The two processes mentioned above are reversible, which is essential in order to explain the tendency of the baked samples to revert toward the characteristics of the air-equilibrated samples over time.

To apply the argument that Ti undergoes a change in coordination upon baking the sample, it must be assumed that the outgassing treatment at 300 °C does not remove all of the water from the zeolite pores. This is necessary since the baked samples revert back to the air-equilibrated samples over time, which requires the presence of water. The assumption is a reasonable one based on thermogravimetric studies of the samples and the fact that temperatures above 300 °C are necessary to fully dehydrate hydrophilic zeolites.

Time-resolved fluorescence of the air-equilibrated sample of TiO_2 in zeolite Y shows two distinct emitting wavelengths, at 440 and 472 nm, which is evidence for the population of two different Ti sites in the sample. Baking of the sample causes a sharpening of the fluorescence band and only one emitting wavelength at 450 nm. This indicates that under the conditions, the solid contains a near-uniform population of Ti sites. On the basis of the argument presented above, the emission at 450 nm must be due to Ti in a "closed" environment, and emission at longer wavelengths must be due to Ti atoms bonded to hydroxyl groups, probably from water acting as a ligand.

The sample of TiO_2 in β zeolite did not show much change in the emission spectrum, even upon heating the sample. The emission wavelength was 450 nm. This suggests that in this case, the TiO_2 clusters are relatively free of hydration water. This explains why there were not many changes upon heating the sample, since there was not much change in the number of hydroxyl groups coordinated with Ti atoms upon the thermal treatment.

The time-resolved fluorescence spectra of TiO_2 included in mordenite contrasted with observations for the sample of TiO_2 in zeolite Y, both in terms of emission intensities and band positions. For the air-equilibrated sample, there was only one fairly broad emission peak, centered at 450 nm. Upon heating of the sample at 300 °C, the emission becomes even broader with two resolvable emission maxima, with more fluorescence intensity at longer wavelengths (>500 nm). We speculate that sample heating resulted in changing the location of the water molecules, causing their relocation and coordination to the Ti, rather than its complete removal. The overall emission intensity for the air-equilibrated sample was less than that for the baked sample, the reverse of what is seen for the other two zeolite samples. This effect reflects the reduced dimensions of the mordenite pores that impose steric restrictions to modifications in the size of the TiO_2 nanoclusters, making them more stable and less prone to the generation of defects.

The lifetimes measured for the zeolite samples, whether baked or air-equilibrated, are comprised of two components. The first component is a short-lived one, with a lifetime ≤200 ps (see Table 1). The second component represents a longer lived species, with a lifetime in the nanosecond range (∼1−1.3 ns). These fast and slow decay lifetimes, which vary somewhat upon sample treatment, probably originate from charge-transfer recombination of shallow and deep sites on the nanocluster, respectively. This has also been observed in femtosecond studies on TiO_2 photocatalytic powders.[43]

Other possible explanations to account for the changes in the spectra observed between the air-equilibrated and baked samples of TiO_2 in zeolites were considered, such as a phase transition of TiO_2 from anatase to rutile. This possibility was rejected, since it has been reported that for TiO_2 particles with a diameter of 3−10 nm, the transition temperature is between 600 and 650 °C, although rutile stabilization was found to occur below 350 °C.[44] These phase transitions seem to occur at much higher temperatures than those used in the present work. A second possibility to be considered is the aggregation of TiO_2 clusters, resulting in an increase in the cluster size. This process, however, seems unlikely to reverse with the elapsed time after baking. Thus, these two possibilities do not appear as a likely explanation for the present results.

Conclusions

The photophysical properties of TiO_2 included in zeolites Y, β, and mordenite have been studied using time-resolved techniques. A blueshift in the ground-state absorption spectra of the zeolite samples compared to bulk anatase was observed and attributed to a direct transition in the semiconductor, rather than a change in the band gap energy due to a size quantization effect. Through time-resolved fluorescence measurements, it was determined that two different Ti sites are present in the nanocluster, depending on sample conditioning: one site consists of Ti in a "closed" environment and the other site has hydroxyl groups bonded to Ti atoms, due

(42) Lu, G.; Linsebigler, A.; Yates, J. T., Jr. *J. Phys. Chem.* **1994**, *98*, 11733.

(43) Furube, A.; Asahi, T.; Masuhara, H.; Yamashita, H.; Anpo, M. *J. Phys. Chem. B* **1999**, *103*, 3120.

(44) Ma, W.; Lu, Z.; Zhang, M. *Appl. Phys. A.* **1998**, *66*, 621.

to the presence of hydration water, which acts as a ligand. The reduction in intensity that is seen upon heating the samples at 300 °C is attributed to the formation of defect sites in the nanocluster, resulting in fewer charge transfer states, and thus a lower emission intensity. These studies are useful to expand upon catalytic studies of TiO_2 nanoclusters in zeolites, since the coordination of Ti will play a crucial role in terms of catalytic activities and efficiencies.

Acknowledgment. J.C.S. thanks the National Sciences and Engineering Research Council of Canada for support, and the Instituto de Tecnología Química (Valencia) where this article was completed while J.C.S was a guest under the auspices (Grant SAB1998-0121) of the Ministerio de Educación y Ciencia (Spain). S.C is the recipient of an NSERC postgraduate scholarship. Financial support from Spanish DGICYT (Grant MAT97-1016-CO2) is also gratefully acknowledged.

CM990679+